Journal of Power Sources 196 (2011) 7886–7890

Contents lists available at ScienceDirect

Journal of Power Sources

journal homepage: www.elsevier.com/locate/jpowsour

Short communication

Constructing a novel and safer energy storing system using a graphite cathode and a MoO_3 anode

Nanda Gunawardhana[a,*], Gum-Jae Park[a], Nikolay Dimov[a], Arjun Kumar Thapa[b], Hiroyoshi Nakamura[c], Hongyu Wang[d], Tatsumi Ishihara[b], Masaki Yoshio[a,*]

[a] Advanced Research Center, Saga University, 1341 Yoga-machi, Saga 840-0047, Japan
[b] Department of Applied Chemistry, Kyushu University, Fukuoka 819-0395, Japan
[c] Department of Chemistry and Applied Chemistry, Saga University, 1 Honjo, Saga 840-8502, Japan
[d] State Key Laboratory Chinese Academy of Sciences, Changchun 130022, China

ARTICLE INFO

Article history:
Received 17 February 2011
Received in revised form 7 April 2011
Accepted 27 April 2011
Available online 5 May 2011

Keywords:
Safety of batteries
Graphite cathode
Molybdenum oxide anode
Intercalation/de-intercalation
Pulse polarization

ABSTRACT

A cell employing a graphite cathode and a molybdenum (VI) oxide (MoO_3) anode is investigated as a possible energy storage device. Graphite cathode allows raising the voltage well above the cathode materials of LIBs without causing safety issues. The bottom potential of this anode is 2.0 V vs. Li/Li^+, which is well above the lithium plating potential. Pulse polarization experiment reveals that no lithium deposition occurs, which further enhances the safety of the graphite/MoO_3 full cell. Charge/discharge mechanism of this system results from intercalation and de-intercalation of the PF_6^- in the cathode (KS-6) and Li^+ in the anode (MoO_3). This mechanism is supported by *in situ* X-ray diffraction data of the graphite/MoO_3 cell recorded at various states of charge.

1. Introduction

Nowadays, rechargeable energy storage systems are attracting growing attention because of increasing fuel costs and environmental issues. Lithium ion batteries (LIB) and electric double-layer capacitors (EDLC) offer promissing alternatives for limiting the use of traditional fossil fuels [1–3]. However, LIB have insufficient power density and safety. Fires caused by LIB have been reported recently [4]. In addition, the electrolyte reacts easily with most cathode materials in their charged state. Charged transition metal cathodes are prone to release oxygen and might trigger dangerous explosion-like reactions [5,6]. On the contrary EDLC do not contain high valence transition metal oxides. Therefore they are considered to be inherently safer. However, EDLC have a considerably smaller energy density due to the lower capacities and working voltages [7–10]. A possible method of increasing the energy density of electrochemical energy storage devices without compromising their safety is by means of so-called hybrid supercapacitors. Hybrid supercapacitors are asymmetrical power sources, in which an electrode of a lithium secondary battery replaces one of the activated carbon electrodes in the EDLC [1,2,10–12,4].

Following a similar approach, we have suggested a novel high-energy capacitor called a Megalo-capacitance capacitor, in which a graphite positive electrode and an activated carbon anode have been used in combination with a Li-free electrolyte [13–15]. The charge storage mechanism at the positive graphite electrode aids in the absorption and intercalation of the PF_6^- anion within the graphite layers. This capacitor provides higher energy density compared with conventional EDLC because of its higher operating voltage and capacity due to not only by adsorption, but also by intercalation [16–18].

Three factors contribute to the safety of these systems. The first factor states that cathode materials used in LIBs are lithiated transition metal oxides, which undergo oxidation to a higher valence state during the charging process. Since there are no transition metal oxides in the positive electrode, there is no possibility for oxygen to be released from the cathode in its over-charged state. Second, the operating voltage of MoO_3 is around 2.0 V vs. Li/Li^+, which is well above the lithium plating potential and the risk of lithium dendride formation is negligible. Third, because both Li^+ and PF_6^- are simultaneously consumed upon charging, the net $LiPF_6$ concentration gradually decreases with the increase of the state of charge. This means that such a device will have a high internal resistance in its overcharged state, which will suppress dangerous high current flow in extreme situations, such as a shortcut or mechanical disintegration.

* Corresponding authors. Tel.: +81 952 20 4729; fax: +81 952 20 4729.
E-mail addresses: kgngu@yahoo.com (N. Gunawardhana), yoshio@cc.saga-u.ac.jp (M. Yoshio).

0378-7753/$ – see front matter © 2011 Elsevier B.V. All rights reserved.
doi:10.1016/j.jpowsour.2011.04.059

Recently, we have demonstrated another electrochemical power source based on graphite and TiO_2 employed as cathode and anode, respectively [17]. However, this system has limited cycle life which might be caused by the TiO_2 anode. To clarify capacity fading mechanism of cells with graphite cathode we have investigated other possible metal oxides to replace TiO_2.

In this work, we describe the features of the power source composed of a KS-6 cathode and MoO_3 anode. *In situ* X-ray diffraction (XRD) measurements performed at various stages of charge of both electrodes were carried out to elucidate the charge storage mechanism. Data obtained from a 4-electrode cell examined the potential profiles of the half-cells Li/MoO_3 and Li/KS-6. They were compared to that of the full cell MoO_3/KS-6 and further confirmed the suggested charge storage mechanism.

2. Experimental

The artificial graphite KS-6 (Timcal, Switzerland) was used for cathode material and commercial MoO_3 (Wako, Japan) was used as anode material. Powder X-ray diffraction (MiniFlex II, Rigaku, Japan) using CuKα radiation was employed to identify the intercalation of anions and structural changes in positive and negative electrodes during charge/discharge cycling. *In situ* XRD analyses were conducted using a homemade cell which was described in a previous report [15]. It was assembled in argon filled glove box to prevent any reaction with moisture in the air and consisted of two electrodes separated by glass fiber filters soaked with electrolyte. The electrodes for *in situ* XRD were prepared by mixing 10 wt% poly(vinylidene-fluoride-hexafluoropropylene)(PVdF-HFP) binder, 80 wt% active material, 10 wt% acetylene black dissolved in N-methyl-2-pyrrolidone (NMP) solution. For the rest of the experiments the electrodes were prepared using 90 wt% active materials with 4 wt% AB (acetylene black) and 6 wt% PVdF binder in NMP solution. The electrochemical characterizations were performed using a CR2032 coin-type cell. The electrodes were pressed under a pressure of 300 kg cm^{-2} and dried at 160 °C for 4 h under vacuum. The positive and negative electrodes were separated by three glass fiber filters and the amount of the electrolyte was ca. 0.5 mL. The electrolyte was 1 M $LiPF_6$-EC:DMC (1:2 by volume) supplied by Ube Chemicals, Japan. Mass loading of electrodes was 4–6 mg cm^{-2}. The charge/discharge performance was carried out in the voltage range of 1.5–3.5 V under a current density of 100 mA g^{-1}.

3. Results and discussion

We have introduced KS-6 as a positive electrode, which belongs to graphite by Franklin definition because the value of the interlayer distance, d(0 0 2), is less than 3.36 Å [19]. Primary use of KS-6 is as a conductive binder. It has an average particle size of around 6 μm and 18 m^2 g^{-1} of specific surface area. The electrochemical properties of KS-6 as anode material in a lithium secondary battery has been studied previously [13–15,17]. The MoO_3 used in this study has an orthorhombic structure with lattice parameters of a = 6.05 Å, b = 29.04 Å, and c = 3.86 Å. Fig. 1 shows the charge/discharge curves of the MoO_3 vs. a Li/Li^+. MoO_3 has voltage plateaus of 2.7 V and 2.4 V at the first charge but the voltage slowly decreases between 2.7 and 2.0 V in the second cycle. Structural change in the crystal lattice of MoO_3 is anticipated during charge/discharge in this voltage range. It shows charge capacities of 228 and 197 mAh g^{-1} at the first and second charge processes. The second discharge capacity decreased by about 5 mAh g^{-1} compared with the first discharge capacity due to the electrolyte decomposition. The retention rate of the discharge capacities was about 90% from the second to the 50th cycle.

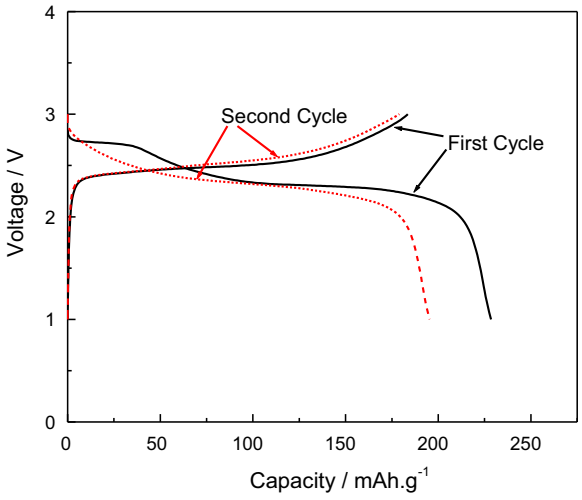

Fig. 1. The initial charge/discharge curves for Li/1 M $LiPF_6$-EC/DMC(1:2)/MoO_3 with a current density of 100 mA g^{-1} between 3.0 and 1.0 V at room temperature.

Pulse polarization experiment of MoO_3 vs. Li/Li^+ was performed in the following manner. The first cycle was carried out at 0.8 mA to form the SEI layer and to measure the capacity of the cell. Then the capacity was changed by predefined increments equal to 20% state of charge (SOC). After adjusting the state of charge, the cell was rested for 5 min and then a pulse of 5 mA with duration of 6 s was applied to the cell. The data is shown in Fig. 2. We use CR2032 coin cells with glass separators soaked with a 1.0 M $LiPF_6$ solution, which typically has an internal resistance associated with the polarization of MoO_3 electrode. It is clear that under current pulse cell voltage remains well above the lithium plating potential.

It is worth noting that only the KS-6/MoO_3 cell allows rising the potential of KS-6 up to 5.5 V vs. Li/Li^+ without significant capacity loss. We were not able to increase the voltage of the cathode up to 5.5 V vs. Li/Li^+ with other metal oxide anodes including TiO_2 reported previously [17]. We believe that partial amophirization of MoO_3 has some influence on the performance of the full cell.

Fig. 3(a) shows the first charge/discharge curve o the KS-6/1M $LiPF_6$-EC/DMC (vol. 1:2)/MoO_3 energy storage system during cycling. In a full cell, the voltage versus capacity curves show bent lines along with linear regions. During the first charging the cell shows a sudden voltage increase up to 2.2 V but the capacity at this stage is small as the amount of the anions adsorbed to the

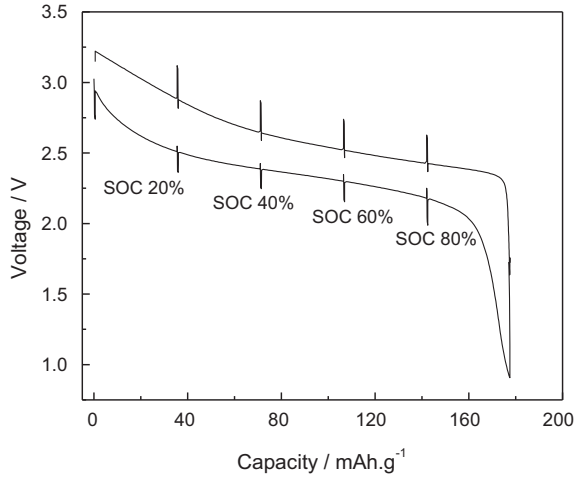

Fig. 2. The result of pulse polarization experiment. The test condition was a current density of 100 mA g^{-1} then a pulse of 500 mA g^{-1} with a duration 6 s.

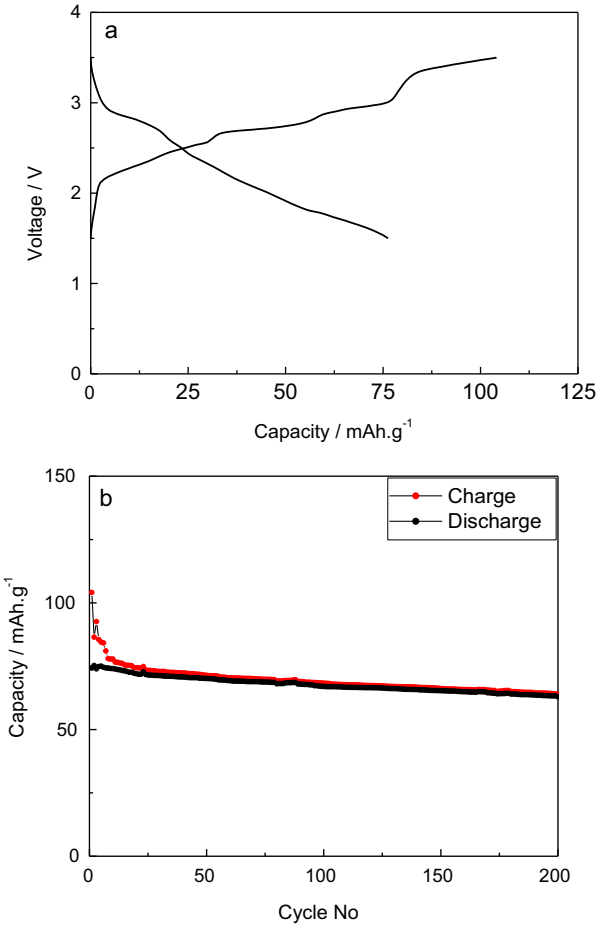

Fig. 3. (a) The initial charge/discharge curves, (b) cycles for the KS-6/MoO_3 cell with an electrode mass ratio of 1:1 in the voltage range of 3.5–1.5 V during cycling. The test condition was a current density of 100 mA g^{-1}.

edge plane regions of the graphite is not large. When the voltage increases further PF_6^- anions start to intercalate within the graphite layers. It is notable that the later process has a major contribution to the overall capacity of the cathode. This mechanism is supported by the *in situ* XRD data. During discharge, the KS-6/MoO_3 cell shows an initial sharp voltage decrease until 2.8 V and then gradually decreases down to 1.5 V. Fig. 3(b) shows the variation in specific charge/discharge capacity with the number of cycles for the KS-6/MoO_3 energy storage system. The KS-6/MoO_3 system shows an initial discharge capacity of 81 mAh g^{-1} and capacity retention of 90% from the 3rd to the 200th cycles. A major factor contributing to the capacity fading of this system is the large volume expansion of graphite during intercalation of PF_6^- anion.

Fig. 4 shows the potential profiles of the KS-6/MoO_3 cell during galvanostatic charge/discharge, recorded in a 4-electrode cell with 2 reference Li electrodes. Such a cell allows measuring the contribution of each half-cell reaction to the overall potential profile. In the initial charge process, the potential of KS-6 jumps suddenly to above 4.5 V against Li metal. Then PF_6^- anions start to insert into the interlayer space of KS-6. This results in the bent shape of the voltage profile, which could be raised up slowly until reaching its ceiling potential. Although some electrolyte decomposition at the KS-6 is observed at high potentials, it is not that drastic like activated carbon, because the specific surface area of KS-6 is rather small. On the other hand, the potential of the MoO_3 negative electrode initially drops down to 2.7 V against Li metal. Then it gradually decreases from 2.7 to 2.0 V against Li metal. These two processes maintain the total voltage of KS-6/MoO_3 between 1.5 and 3.5 V.

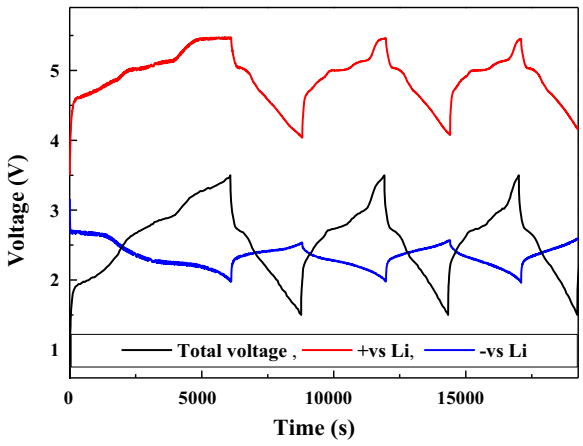

Fig. 4. Potential profiles of KS-6/MoO_3 cell during the galvanostatic charge/discharge process. The positive and negative electrodes have the same weight of active material.

In order to investigate the reaction mechanism and structural changes of the cathode and the anode, *in situ* XRD experiments were conducted. Fig. 5(a) shows *in situ* XRD diffractions of the KS-6 electrode in the KS-6/MoO_3 energy storage cell at various voltages. The (0 0 2) peak at 26.5° corresponding to a 3.35 Å value for d(0 0 2) indicated a well-ordered graphitic structure. The (0 0 2) peak started to shift to a lower angle at 2.0 V (4.5 V vs. Li/Li^+) and then the peak split into two peaks at 24.3° and 25.3° during the voltage change from 2.0 to 3.5 V.

KS-6/MoO_3 allows rising the potential of KS-6 up to 5.5 V vs. Li/Li^+, which is 0.2 V higher than the cathode of KS-6/TiO_2 cell. Under such a higher potential PF_6^- can intercalate deeper into the graphite structure. Deeper PF_6^- intercalation results in a stronger peak position at 24.3°. Seel and Dahn have studied the intercalation of PF_6^- anion into graphite. They have observed a peak in XRD spectra at 25.3° which corresponds to gallery height of 4.5 Å [20]. In the present work we observe this peak at 25.2° which corresponds to gallery height of 4.6 Å. According to the literature the stage numbers for anion intercalation into the KS-6 can be roughly estimated as 3 and 5, respectively [21–25]. Since stage 3 is dominant, we can extract higher capacity from KS-6 compared to the KS-6/TiO_2 cell. We believe that ascription of stage number needs further investigation. We will continue to study the stage structure in the near future. During the first discharge peak position of electrode change back to 26.5°. However, the peak intensity is relatively small compared to that of the pristine material.

Fig. 5(b) shows the *in situ* XRD patterns of MoO_3 in the KS-6/MoO_3 energy storage system. Unlike graphite, MoO_3 peak shift has started at 2.0 V (2.7 V vs. Li/Li^+) and the original peaks disappeared at the end of charge. It can be assumed that the capacity of MoO_3 is larger than the other tested metal oxides (TiO_2 and Nb_2O_5) and results in a structural change from orthorhombic to amorphous state [17]. This was confirmed by discharging the full cell back to zero volts. Unlike graphite, the original peak positions and heights of MoO_3 do not reappear in the XRD pattern which indicates its partial amorphization [26]. Despite this amorphization, it is the most stable metal oxide tested so far to construct a full cell. Though the potential of the full cell is increased up to 3.5 V, as we observed from the 4-electrode cell, the voltage of MoO_3 anode only changes from 2.7 to 2.0 V vs. Li/Li^+. The *in situ* XRD and 4-electrode cell results could be used to elucidate the intercalation mechanism of $LiPF_6$ into graphite and MoO_3 when the weight ratio of cathode to anode is 1:1. During the charging of the KS-6/MoO_3 full cell, the ions in the $LiPF_6$ electrolyte solution migrate towards their respective electrodes. The PF_6^- ions intercalate into the interlayer spaces

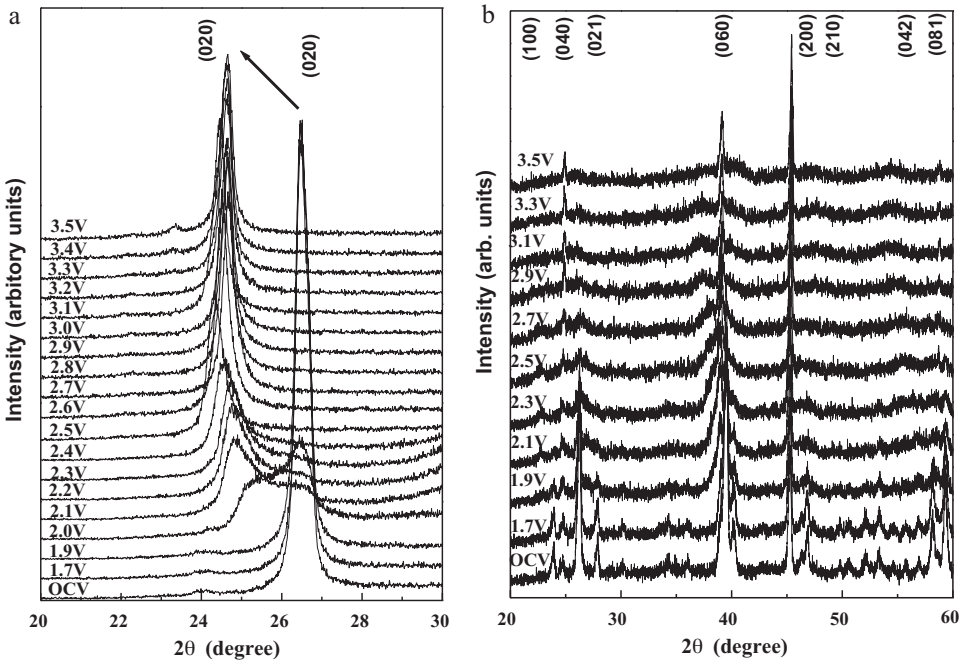

Fig. 5. *In situ* XRD patterns of the (a) KS_6 (graphite) and the (b) MoO_3 electrode during the first charging process of a KS_6/MoO_3 energy storage system with a weight ratio of 1:1 for KS_6 to MoO_3.

of the graphite cathode electrode, while the Li^+ ions insert into the MoO_3 anode. The first part of the mechanism takes place in the voltage region from 0 to 2.2 V in the charging process and involves adsorption of PF_6^- to the edge-plane surfaces of graphite. The second part of the mechanism proceeds when potential exceeds 2.0 V and involves PF_6^- intercalation into KS-6. When the KS-6/MoO_3 cell is discharged, the Li^+ and PF_6^- ions are extracted from their respective electrode structures and reconstituted into the original $LiPF_6$ solution. These types of electrochemical devices do not fall into any of the existing categories of capacitors and rechargeable batteries. This kind of electrochemical cell shows merits in the concepts of safety and high-energy density compared with Li-ion batteries and EDLC, respectively.

In the present study, we investigate the performance of KS-6/MoO_3 by using a weight ratio of cathode to anode material of 1:1. In addition, we used a 1.0 M $LiPF_6$ solution as the electrolyte. We suggest that performance of this energy storage system could improve by changing the weight ratios of the cathode to anode and the concentration of the electrolyte. This is because energy density, swing voltage, and specific capacitance are functions of the electrodes mass ratio and ion concentration of the electrolyte. As the overall performance, including capacity and cycleability, depends on the matching ratio between positive and negative electrodes, we will continue to study this area in future to enhance the performance of KS-6/MoO_3 energy storage system. Furthermore, we will continue to study the intercalation of different anions such as BF_4^-. The latter is smaller than PF_6^-. Therefore it may exhibit deeper intercalation into the interlayer spacing of graphite, giving a higher capacity while preserving the good cycleability of the MoO_3/KS-6 cell.

4. Conclusions

A novel energy storage system containing a graphite cathode and MoO_3 anode has a high capacity, as well as a good cycleability in the voltage region between 1.5 and 3.5 V. During charging, KS-6 undergoes deeper PF_6^- intercalation compared with other KS-6/(metal oxide) cells. *In situ* X-ray data, reveal that deeper intercalation of PF_6^- into the graphite cathode leads to some structural changes of the pristine graphite structure. The MoO_3 anode undergoes partial amorphization. Despite its amorphization, MoO_3 generates the most stable life cycle. Such electrochemical storage systems are inherently safe because there are no transition metal oxides at their higher valence state. In addition overcharge is not possible because the electrolyte is being gradually consumed upon charging.

Acknowledgment

Partial financial support from Fukuoka Industrial Science Foundation is gratefully acknowledged.

References

[1] W. Fergus, J. Power Sources 195 (2010) 939.
[2] B. Peng, J. Chen, Coord. Chem. Rev. 253 (2009) 2805.
[3] A. Lewandowski, M. Galinski, J. Power Sources 173 (2007) 822.
[4] H. Arai, M. Tsuda, K. Saito, M. Hayashi, Y. Sakurai, J. Electrochem. Soc. 149 (2002) A401.
[5] B.E. Conway, Electrochemical Sypercapacitor-Scientific Fundamentals and Technologicla Application, Kluwer Academic, New York, 1999, pp. 29–31.
[6] A. Burke, J. Power Sources 91 (2000) 37.
[7] O. Barbieri, M. Hahn, A. Herzog, R. Kotz, Carbon 43 (2005) 1303.
[8] M. Hahn, A. Warsig, R. Gallay, P. Novak, R. Kotz, Electrochem. Commun. 7 (2005) 925.
[9] D.H. Jurcakova, M. Seredych, Y. Jin, G.Q. Lu, T.J. Bandosz, Carbon 48 (2010) 1767.
[10] S.S. Zhang, K. Xu, T.R. Jow, J. Power Sources 160 (2006) 1349.
[11] W. Sugimoto, H. Iwata, Y. Yasunaga, Y. Murakami, Y. Takasu, Angew. Chem. 115 (2003) 4226.
[12] G.G. Amatucci, F. Badway, A. Dupsquier, T. Zheng, J. Electrochem. Soc. 148 (2001) A930.
[13] M. Yoshio, H. Nakamura, H. Wang, Electrochem. Solid States Lett. 9 (2006) A561.
[14] H. Wang, M. Yoshio, Electrochem. Commun. 8 (2006) 1481.
[15] H. Wang, M. Yoshio, A.K. Thapa, H. Nakamura, J. Power sources 169 (2007) 365.
[16] H. Wang, M. Yoshio, J. Power Sources 171 (2008) 681.
[17] A.K. Thapa, G. Park, H. Nakamura, T. Ishihara, N. Moriyama, T. Kawamura, H. Wang, M. Yoshio, Electrochim. Acta 55 (2010) 7305.
[18] G. Park, D. Kalpana, A.K. Thapa, H. Nakamura, Y.-S. Lee, M. Yoshio, Bull. Korean Chem. Soc. 30 (2009) 817.
[19] R.E. Franklin, Acta Crystallogr. 4 (1951) 235.
[20] J.A. Seel, J.R. Dhan, J. Electrochem. Soc. 147 (2000) 892.
[21] N. Koshiba, K. Takata, M. Nakanishi, Z. Takehara, Denki kaguku 62 (1994) 631.
[22] D. Aurbach, H. Teller, M. Koltypin, E. Levi, J. Power Sources 1 (2003) 119.

[23] M. Holzapfel, H. Buqa, F. Krumeich, P. Novak, F.M. Petrat, C. Veit, Electrochem. Solid State Lett. 8 (2005) A516.
[24] P.W. Ruch, M. Hahn, F. Rosciano, M. Holzapfel, H. Kaiser, W. Scheifele, B. Schmitt, P. Novak, R. Kotz, A. Wokaun, Electrochim. Acta 53 (2007) 1074.
[25] N. Bartlet, B.W. Mcquillan, Graphite chemistry, in: M.S. Whittingham, A.J. Jacobson (Eds.), Intercalation Chemistry, Accedemic Press, New York, 1982, pp. 19–50.
[26] J.O. Besenhard, J. Heydecke, H.P. Fritz, Solid State Ionics 6 (1982) 215.